ИЗВЕСТИЯ ВЫСШИХ УЧЕБНЫХ ЗАВЕДЕНИЙ.
Т 69 (8) Серия «**ХИМИЯ И ХИМИЧЕСКАЯ ТЕХНОЛОГИЯ**» 2026
V 69 (8) **ChemChemTech** 2026

DOI: 10.6060/ivkkt.20266908.7170
УДК: 537.528+541.15

СИНТЕЗ СЛОИСТОГО ГИДРООКСИДА ЭРБИЯ ПОД ДЕЙСТВИЕМ РАЗРЯДА ПОСТОЯННОГО ТОКА НА ВОДНЫЙ РАСТВОР НИТРАТА ЭРБИЯ

А.В. Сунгурова, А.Н. Иванов, А.А. Куколь, В.Ю. Панин, В.В. Рыбкин

Александр Николаевич Иванов (ORCID 0000-0002-5207-7582), Владимир Владимирович Рыбкин (ORCID 0000-0001-7295-7803)*

Кафедра технологии приборов и материалов электронной техники, Ивановский государственный химико-технологический университет, Шереметевский пр., 7, Иваново, Российская Федерация, 153000
E-mail: rybkin@isuct.ru*

Андрей Александрович Куколь, Виктор Юрьевич Панин, Александра Вадимовна Сунгурова (ORCID 0000-0002-2406-6165)

Кафедра промышленной экологии, Ивановский государственный химико-технологический университет, Шереметевский пр., 7, Иваново, Российская Федерация, 153000

Впервые исследована кинетика образования гидрооксида эрбия при действии на водный раствор его нитратов разряда постоянного тока в воздухе. Диапазон исследованных концентраций нитратов составлял (5-40) ммоль/л, а токов разряда (40-80) мА. Показано, что образование гидрооксида происходит только в случае, когда раствор является анодом. В этом случае действие разряда приводит к росту pH раствора и достигается концентрация ионов OH-, необходимая для образования осадка гидрооксида. Определены формальные константы скоростей образования гидрооксида и степени превращения ионов Er^{3+} при разных токах разряда. Константы скорости зависели от тока разряда и начальной концентрации. При заданном токе разряда константы скорости росли с ростом начальной концентрации. При токе разряда 80 мА константы менялись от $2{,}1\cdot10^{-3}$ до $7{,}7\cdot10^{-3}$ c^{-1} при увеличении концентрации от 5 до 40 ммоль/л. При этом степени превращения Er^{3+} уменьшались от 0,58 до 0,32, а энергетические выходы увеличивались от $7{,}6\cdot10^{-2}$ до 0,86 ионов на 100 эВ вложенной энергии. Методом динамического рассеяния света обнаружено, что полученный гидрооксид образует две фракции с гидродинамическим диаметром частиц (45,5±5,2) нм и (582±85) нм. Содержание первой фракции (43±2)%, а второй – (57±2)%. Химический состав продукта, определенный методом ЭДС, соответствует формуле $[Er_2(OH)_5](NO_3)\cdot5H_2O$. То есть полученное вещество относится к слоистым двойным гидроксидам. Эти вещества состоят из положительно заряженных слоев гидроксидов редкоземельных элементов и отрицательно заряженных межслойных анионов. СЭМ фотографии подтверждают это заключение.

Ключевые слова: эрбий, гидрооксид, синтез, разряд, кинетика

Для цитирования:
Сунгурова А.В., Иванов А.Н., Куколь А.А., Панин В.Ю., Рыбкин В.В. Синтез слоистого гидрооксида эрбия под действием разряда постоянного тока на водный раствор нитрата эрбия. *Изв. вузов. Химия и хим. технология*. 2026. Т. 69. Вып. 8. С. 6–11. DOI: 10.6060/ivkkt.20266908.7170.

For citation:
Sungurova A.V., Ivanov A.N., Kukol A.A., Panin V.Yu., Rybkin V.V. Synthesis of layered erbium hydroxide under the action of direct current discharge on an aqueous solution of erbium nitrate. *ChemChemTech* [*Izv. Vyssh. Uchebn. Zaved. Khim. Khim. Tekhnol.*]. 2026. V. 69. N 8. P. 6–11. DOI: 10.6060/ivkkt.20266908.7170.

SYNTHESIS OF LAYERED ERBIUM HYDROXIDE UNDER THE ACTION OF DIRECT CURRENT DISCHARGE ON AN AQUEOUS SOLUTION OF ERBIUM NITRATE

A.V. Sungurova, A.N. Ivanov, A.A. Kukol, V.Yu. Panin, V.V. Rybkin

Alexander N. Ivanov (ORCID 0000-0002-5207-7582), Vladimir V. Rybkin (ORCID 0000-0001-7295-7803)*

Department of Microelectronic Devices and Materials, Ivanovo State University of Chemistry and Technology, Sheremetevsky ave., 7, Ivanovo, 153000, Russia
E-mail: rybkin@isuct.ru*

Andrey A. Kukol, Viktor Yu. Panin, Alexandra V. Sungurova (ORCID 0000-0002-2406-6165)

Department of Industrial Ecology, Ivanovo State University of Chemistry and Technology, Sheremetevsky ave., 7, Ivanovo, 153000, Russia

The kinetics of erbium hydroxide formation under the action of a direct current discharge in air on an aqueous solution of its nitrates was studied for the first time. The range of studied nitrate concentrations was (5-40) mmol/L, and discharge currents (40-80) mA. It was shown that hydroxide formation occurs only when the solution is anode. In this case, the discharge leads to an increase in the pH of the solution and the concentration of OH- ions required for the formation of a hydroxide precipitate is achieved. Formal rate constants of hydroxide formation and the degrees of conversion of Er^{3+} ions were determined at different discharge currents. The rate constants depended on the discharge current and the initial concentration. For a given discharge current, the rate constants increased with increasing initial concentration. At a discharge current of 80 mA, the constants varied from $2.1 \cdot 10^{-3}$ to $7.7 \cdot 10^{-3}$ s^{-1} with an increase in concentration from 5 to 40 mmol/L. In this case, the Er3+ conversion rates decreased from 0.58 to 0.32, while the energy yields increased from 7.6·10-2 to 0.86 ions per 100 eV of input energy. Using dynamic light scattering, it was found that the resulting hydroxide forms two fractions with hydrodynamic particle diameters of (45.5±5.2) nm and (582±85) nm. The content of the first fraction is (43±2)%, and the second is (57±2)%. The chemical composition of the product, determined by the EDS method, corresponds to the formula $[Er_2(OH)_5](NO_3) \cdot 5H_2O$. That is, the obtained substance belongs to layered double hydroxides. These substances consist of positively charged layers of rare earth element hydroxides and negatively charged interlayer anions. SEM images confirm this conclusion.

Keywords: erbium, hydroxide, synthesis, discharge, kinetics

INTRODUCTION

Layered anion-exchange compounds are attracting considerable interest in many areas of chemistry. In particular, the cleavage of crystalline layered solids into individual layers allows the production of molecularly thin two-dimensional (2D) materials [1]. This type of materials includes layered rare earth element (REE) hydroxides, which combine the ability to exchange anions with the interesting properties of REEs. In these substances, a cationic two-dimensional lattice is formed from the $REE(OH)_3$ crystalline framework through dimensionality reduction and topological engineering. Subsequent chemical exfoliation leads to the formation of REE-based hydroxide nanosheets. Interest in these compounds is associated with their catalytic and photoluminescent properties, as well as biomedical applications [2-4].

Most frequently (~70%), either hydrothermal precipitation [5] or chemical precipitation [6] are used to obtain REE hydroxides. The main disadvantages of these methods are elevated temperatures (100 °C and above) and pressures, as well as the duration of the process (hours and tens of hours). The presence of precipitating reagents also does not contribute to the purity of the product. In this paper, we investigate the possibilities of obtaining REE by a relatively new method, which we first used in [7] for the synthesis of $Zn(OH)_2$. The method involves the action of a direct current gas discharge at atmospheric pressure in air on an aqueous solution of erbium nitrate. And this method does not have the above-mentioned disadvantages. The object of the study was erbium hydroxide ($Er(OH)_3$). This choice was due to the fact that, according to a literature analysis [4], out of 216 papers published before 2022, only 5 were devoted to erbium.

EXPERIMENTAL PART

The reactor consisted of two glass cells separated by a cellophane membrane (Fig. 1). Each cell had a volume of 80 ml. High voltage was applied to titanium electrodes located 4 mm above the solution surface so that one cell served as a liquid anode and the other as a liquid cathode. The discharge was initiated in air at atmospheric pressure, with a discharge current of 40-80 mA. Aqueous nitrate solutions were prepared by dissolving analytical-grade $Er(NO_3)_3 \cdot 5H_2O$ in distilled water. Solution concentrations were 5-40 mmol/L (calculated as erbium).

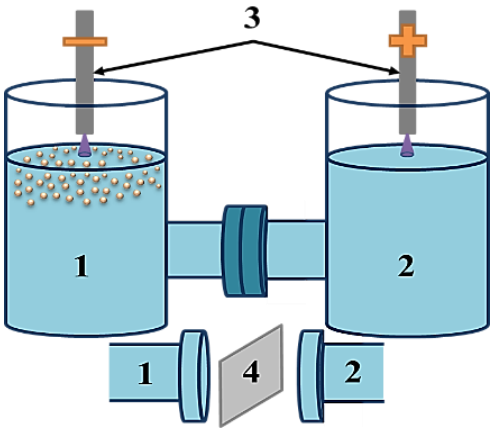

Fig. 1. Schematic diagram of the experimental setup. 1 – liquid anode, 2 – liquid cathode, 3 – titanium electrodes, 4 – cellophane membrane

Рис. 1. Схема экспериментальной установки. 1 – жидкий анод, 2 – жидкий катод, 3 – титановые электроды, 4 – целлофановая мембрана

After a certain discharge exposure time, the Er^{3+} ion concentration and pH of the solution were determined. The pH of the solution was measured using a PHT-028 water quality analyzer (Kelilong, China), and the Er^{3+} ion concentration was determined using the complexometric titration method described in [8]. The maximum discharge burn time was 600 s. Each measurement was performed at least five times, with the average value and standard error determined.

To determine the power input into the discharge at a given current, the voltage drop between the metal electrodes was measured using a TrueRMSFluke 280 precision voltmeter.

As the discharge burned, a pink colloidal solution began to form in the upper part of the anode cell. This color is characteristic of erbium hydroxide [9]. Over time, the solution lost its aggregative stability, and a precipitate settled at the bottom of the cell. The precipitate was filtered and washed five times with distilled water. The resulting substance was air-dried at 50 °C for 24 h and analyzed.

The colloidal solution was used to determine the hydrodynamic sizes of particles using dynamic light scattering (DLS: Photocor Compact –Z, Russia).

The surface microstructure of the synthesized substance was studied using scanning electron microscopy (SEM: Tescan Vega 3SBH, Czech Republic). The elemental composition of the powders was determined using energy-dispersive spectroscopy (EDS: Aztec EDS, Oxford Instruments Ltd., England).

RESULTS AND DISCUTION

A typical kinetic dependence of the concentration of Er^{3+} ions and the degree of their conversion is shown in Fig. 2.

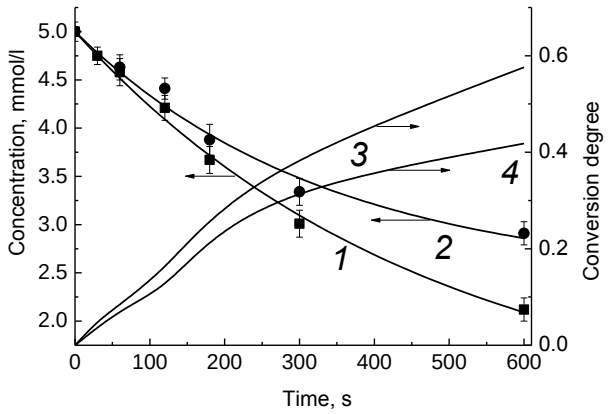

Fig. 2. Kinetics of changes in the concentration of erbium ions (*1,2*) and their degree of conversion (*3,4*) in the liquid anode. *1,3* – current 80 mA. *2,4* – current 40 mA

Рис. 2. Кинетика изменения концентрации ионов эрбия (*1,2*) и их степени превращения (*3,4*) в жидком аноде. *1,3* –ток 80 мА. *2,4* – ток 40 мА

Measurements showed that a colloidal solution does not form in the liquid cathode under the action of a discharge, and the concentration of Er^{3+} ions does not change during the experiment.

By processing the kinetic curves in various ways, we came to the conclusion that the best option (determination coefficient R^2 0.98 and higher) corresponds to the following dependence of concentration C on time t:

$$C(t) = \alpha + \beta \cdot \exp(-K \cdot t). \quad (1)$$

This expression corresponds to the kinetic law

$$\frac{dC}{dt} = -K \cdot C + W, \quad (2)$$

where K is the apparent rate constant of ion loss, W is the rate of their formation, and the constants α and β are defined as $\alpha = W/K$ and $\beta = (C_0\text{-}W/K)$, where C_0 is the initial concentration of ions (at $t = 0$).

The results of processing the kinetic dependencies allow us to determine the values of K and W. These data are presented in Table 1.

Table 1

Kinetic parameters of Er^{3+} ion conversion
***Таблица 1.* Кинетические параметры конверсии ионов Er^{3+}**

Concentration, mmol/l	Discharge current is 80 mA		Discharge current is 40 mA	
	K, s^{-1}	W, mmol/(l·s)	K, s^{-1}	W, mmol/(l·s)
5	$(2.1\pm0.6)\cdot10^{-3}$	$(2.1\pm0.6)\cdot10^{-3}$	$(3.0\pm0.2)\cdot10^{-3}$	$(7.2\pm1)\cdot10^{-3}$
20	$(5.8\pm1.0)\cdot10^{-4}$	$(1.0\pm0.2)\cdot10^{-1}$	$(1.1\pm0.3)\cdot10^{-3}$	$(1.1\pm0.3)\cdot10^{-2}$
40	$(7.7\pm0.6)\cdot10^{-3}$	$(2.1\pm0.2)\cdot10^{-1}$	$(5.5\pm0.5)\cdot10^{-3}$	$(1.7\pm0.2)\cdot10^{-1}$

Using the same data, we determined the energy parameters of the process (the number of converted ions per 100 eV of input energy (φ)) and the degree of ion conversion (α). The results are shown in Table 2. The value of φ was calculated for the processing time $t = K^{-1}$ as proposed in [10]:

$$\varphi = \frac{[C_0 - C(t)]\cdot V_V \cdot N_{AV} \cdot e \cdot 100}{P \cdot t} \qquad (3)$$

where C_0 and $C(t)$ are concentrations (mol/l), V_V is the cell volume (0.08 l), N_{AV} is Avogadro's constant, e is the electron charge (C), P is the power input into the discharge (W).

The value of α was calculated as

$$\alpha = \frac{C_0 - C(t=600\,c)}{C_0} \qquad (4)$$

Table 2

Degrees of conversion and energy yields of the Er^{3+} ion conversion process
***Таблица 2.* Степени превращения и энергетические выходы процесса конверсии ионов Er^{3+}**

Concentration, mmol/l	Discharge current is 80 mA		Discharge current is 40 mA	
	Degree of transformation during 600 s, α	Energy output, ions/100 eV, φ	Degree of transformation during 600 s, α	Energy output, ions/100 eV, φ
5	0.58	$7.6\cdot10^{-2}$	0.42	$1.0\cdot10^{-2}$
20	0.22	$9.4\cdot10^{-2}$	0.12	$1.3\cdot10^{-1}$
40	0.32	$8.6\cdot10^{-1}$	0.24	$7.7\cdot10^{-1}$

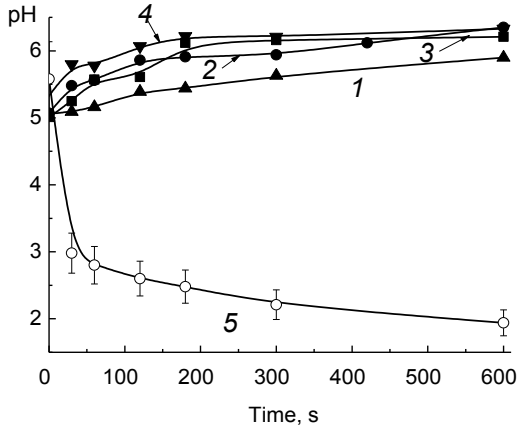

Fig. 3. Dependence of solution pH on treatment time in the liquid anode (*1-4*) and cathode (5). *1, 3* – 40 mA. *2, 4, 5* – 80 mA. *2, 3* – 20 mmol/l. *1, 4, 5* – 40 mmol/l

Рис. 3. Зависимость pH раствора от времени обработки в жидком аноде (*1-4*) и катоде (5). *1, 3* – 40 мА. *2, 4, 5* – 80 мА. *2, 3* – 20 ммоль/л. *1, 4, 5* – 40 ммоль/л

As noted, the process occurs in the surface layer, the depth of which is significantly shallower than the depth of the solution. Therefore, it can be assumed that W is the rate of ion influx into the reaction zone from the depth of the solution. This rate is determined by the diffusion and drift of Er^{3+} ions in the electric field. Therefore, it can be expected that, for a given discharge current, the diffusion component will increase with increasing initial concentration. And, for a given concentration, the drift component will increase with increasing discharge current. This is indeed generally observed (Table 1).

The dependence of the constants on concentration indicates that these constants are apparent. For a given discharge current, which ensures a constant flow of active particles from the discharge to the solution surface, the change in the constants with concentration indicates that reactions involving the solute, despite low concentrations, also influence the formation and destruction of active particles in the solution. This is also evidenced by the kinetics of the solution's pH (Fig. 3).

In the liquid cathode, in contrast to the anode, the pH of the solution always decreases from ~5 to ~2 (at 600 s), and the values themselves depend weakly on the concentration and current. The increase in the pH of the solution is apparently the reason for the formation of hydroxide. Indeed, the solubility product for $Er(OH)_3$ is equal to $(1.63 \pm 0.17)\cdot10^{-26}$ [11]. Calculation using this value shows that, for equilibrium conditions, the formation of hydroxide will be observed when pH equals 5.2 and 5.3 for $[Er^{3+}]$ concentrations

of 40 and 20 mmol/l, respectively. For these reasons, hydroxide formation occurs in the anode, but no formation is observed in the cathode. The differences in pH values are mainly due to differences in the mechanisms of formation of H^+ and OH^- ions in the liquid cathode and anode. This mechanism was studied and described in detail in [12]. The main reason for the increase in pH in the anodic part is that the anode is subjected to bombardment by electrons from the discharge. These electrons, being solvated, react at a high rate with water molecules, forming OH^- ions ($e_{eq} + H_2O \rightarrow \rightarrow 0.5H_2 + OH^-$, $K = 5.5 \cdot 10^9$ l/(mol·s)) [13,14]. We also note that similar kinetic dependences with close rate constants, rates, degrees of conversion and energy yields are observed during the formation of cobalt hydroxide ($Co(OH)_2$) under the action of a discharge on an aqueous solution of its nitrates at the same concentrations and discharge currents [15]. Unfortunately, it is not possible to conduct similar comparisons with other synthesis methods, since none of the works known to us provides data on the precipitation kinetics and product yields.

The results of the DLS analysis showed that after a discharge action time of 600 s, the colloidal solution formed consists of two fractions. One fraction has an average hydrodynamic particle diameter of (45.5±5.2) nm, and the other - (582±85) nm. The content of the first fraction is (43±2)%, and the second - (57±2)%. Apparently, the first fraction is primarily formed colloidal particles, and the second fraction is the result of coagulation of primary particles. It can be said that the formation of two fractions is a general pattern for the processes of hydroxide formation under the action of discharges on aqueous solutions of metal salts. Thus, such a phenomenon was observed in the synthesis of $Cd(OH)_2$ from $Cd(NO_3)_2$ solutions [16, 19], $Cu(OH)_2$ from $Cu(NO_3)_2$ solution [17], $Ni(OH)_2$ from $Ni(NO_3)_2$ solution [18].

Elemental analysis of the obtained substance showed that its chemical formula can be described as $[Er_2(OH)_5](NO_3) \cdot 5H_2O$. The best known categories of such substances are layered double hydroxides (LDH), which are also called anionic clay materials [20–21]. With respect to rare earth elements (RE), they have the general formula $[RE_2(OH)_{6-m}](A^{n-})_{m/n} \cdot xH_2O$ (m = 1 or 2; A^{n-} is the n-valent anion). These substances consist of positively charged layers of rare earth hydroxides and negatively charged interlayer anions. The main layers and guest anions are linked by strong chemical bonds between RE^{3+} cations and interlayer anions, which leads to anion-exchange properties [22,23]. The SEM image of the obtained substance (Fig. 4) shows that the formation of agglomerates in the form of lamellar structures (layers) actually occurs.

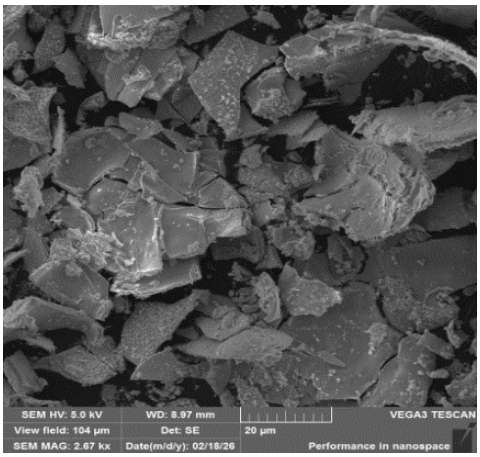

Fig. 4. SEM image of the synthesized substance
Рис. 4. СЭМ вид синтезированного вещества

CONCLUSION

Thus, this article demonstrates the feasibility of producing layered nanoscale erbium hydroxides by exposing an aqueous solution of erbium nitrate to a direct current discharge at atmospheric pressure in air. Unlike other traditional synthesis methods, this method does not require any precipitating reagents, and the process itself occurs in a short time (approximately 10 minutes).

The work was supported by the Ministry of Higher Education and Science of the RF, project no. FZZW- 2026-0005.

The authors declare the absence of a conflict of interest warranting disclosure in this article.

Работа выполнена при поддержке Министерства высшего образования и науки РФ, проект № FZZW-2026-0005.

Авторы заявляют об отсутствии конфликта интересов, требующего раскрытия в данной статье.

REFERENCES
ЛИТЕРАТУРА

1. **Liang J., Ma R., Sasaki T.** Layered rare-earth hydroxides: crystal engineering toward functional nanosheets. *Trends Chem*. 2023. V. 5. N 11. P. 799-813. DOI: 10.1016/j.trechm.2023.09.004.
2. **Bai M., Wan H., Zhang Y., Chen S., Lu C., Liu X., Chen G., Zhang N., Ma R.** Two-dimensional nanomaterials based on rare earth elements for biomedical applications. *Chem. Sci.* 2024. V. 15. P. 16887-16907. DOI: 10.1039/d4sc02625j.
3. **Boumeriame H., Da Silva E.S., Cherevan A.S., Chafik T., Faria J.L., Eder D.** Layered double hydroxide (LDH)-based materials: A mini-review on strategies to improve the performance for photocatalytic water splitting. *J. Energy Chem*. 2022. V. 63. P. 406-432. DOI: 10.1016/j.jechem.2021.04.050.

4. **Seliverstov E.S., Golovin S.N., Lebedeva O.E.** Layered Double Hydroxides Containing Rare Earth Cations: Synthesis and Applications. *Front. Chem. Eng.* 2022. V. 4. 867615. P. 1-8. DOI: 10.3389/fceng.2022.86761.
5. **Assaaoudi H., Fang Z., Butler I.S., Kozinski J.A.** Synthesis of erbium hydroxide microflowers and nanostructures in subcritical water. *Nanotechnology.* 2008. V. 19. P. 185606. DOI: 10.1088/0957-4484/19/18/185606.
6. **Dong X., Hong G.** Preparation of Rare Earth Hydroxide and Oxide Nanoparticles by Precipitation Method. *J. Mater. Sci. Technol.* 2005. V. 21. N 4. P. 555-558.
7. **Shutov D.A., Rybkin V.V., Ivanov A.N., Smirnova K.V.** Synthesis of Zinc Oxide Powders in Plasma–Solution Systems. *High Energy Chem.* 2017. V. 51. N 1. P. 65-69. DOI: 10.1134/S0018143917010118.
8. **Рябухин В.А., Рябчиков Д.И.** Аналитическая химия редкоземельных элементов и иттрия. Серия «Аналитическая химия элементов». М.: Наука. 1966. 380 с. **Ryabukhin V.A., Ryabchikov D.I.** Analytical chemistry of rare earth elements and yttrium. Series "Analytical chemistry of elements". M.: Nauka. 1966. 380 p. (in Russian).
9. **Васильева А.В., Гетьман А.А.** Эрбий и его применение в современной технике. *Литье и металлургия*. 2017. Т. 3. С. 95-96. DOI: 10.21122/1683-6065-2017-3. **Vasilyeva A.V., Getman A.A.** Erbium and its use in modern technology. *Casting and metallurgy.* 2017. V. 3. P. 95-96 (in Russian). DOI: 10.21122/1683-6065-2017-3
10. **Rybkin V.V., Bobkova E.S.** Peculiarities of Energy Efficiency Comparison of Plasma Chemical Reactors for Water Purification from Organic Substances. *Plasma Chem. Plasma Process.* 2015. V. 35. N 1. P. 133-142. DOI 10.1007/s11090-014-9583-8.
11. **Чиркст Д.Э., Лобачёва О.Л., Берлинский И.В., Левичев С.А.** Термодинамическое исследование ионной флотации эрбия(III). *Вест. Санкт-Петербургского Универ.* 2009. Сер. 4. Вып. 4. С. 89-94. **Chirkst D.E., Lobacheva O.L., Berlinsky I.V., Levichev S.A.** Thermodynamic study of erbium(III) ion flotation. *Vest. St. Petersburg Univer.* 2009. Ser. 4. Iss. 4. P. 89-94 (in Russian).
12. **Shutov D.A., Smirnova K.V., Ivanov A.N., Rybkin V.V.** The Chemical Composition of Species Formed in a Water Anode Under the Action of a Direct Current Electric Discharge: Comparison with Liquid Cathode—Experiment and Simulation. *Plasma Chem. Plasma Process.* 2023. V. 43. N 3. P. 577–597. DOI: 10.1007/s11090-023-10322-1.
13. **Witzke M., Rumbach P., David B., Go D.B., Sankaran R.M.** Evidence for the electrolysis of water by atmospheric-pressure plasmas formed at the surface of aqueous solutions. *J. Phys. D: Appl. Phys.* 2012. V. 45. N 44. P. 442001. DOI: 10.1088/0022-3727/45/44/442001.
14. **Rumbach P., Bartels D.M., Sankaran R.M., Go D.B.** The solvation of electrons by an atmospheric-pressure plasma. *Nat. Commun.* 2015. V. 6. N 1. P. 7248. DOI: 10.1038/ncomms8248.
15. **Smirnova K.V., Shutov D.A., Ivanov A.N., Manukyan A.S., Rybkin V.V.** Plasma-solution synthesis of cobalt oxides. *Phys. Scr.* 2024. V. 99. N 7. P. 075031. DOI: 10.1088/1402-4896/ad55b5.
16. **Shutov D.A., Smirnova K.V., Gromov M.V., Ivanov A.N., Rybkin V.V.** Synthesis of CdO Ultradisperse Powders Using Atmospheric Pressure Glow Discharge in Contact With Solution and the Investigation of Intermediate Products. *Plasma Chem. Plasma Process.* 2018. V. 38. N 1. P. 107–121. DOI: 10.1007/s11090-017-9856-0.
17. **Shutov D.A., Smirnova K.V., Ivanov A.N., Rybkin V.V.** Factors Governing the Formation of Oxygen−Containing Copper Powders in a Plasma−Solution System. *Plasma Chem. Plasma Process.* 2022. V. 42. N 1. P. 1-12. DOI: 10.1007/s11090-021-10208-0.
18. **Смирнова К.В., Извекова А.А., Шутов Д.А., Иванов А.Н., Манукян А.С., Рыбкин В.В.** Плазменно-растворный синтез никельсодержащих порошков под действием тлеющего разряда постоянного тока. *Изв. вузов. Химия и хим. технология*. 2022. Т. 65. Вып. 12. С. 112-118. DOI: 10.6060/ivkkt.20226512.6743. **Smirnova K.V., Izvekova A.A., Shutov D.A., Ivanov A .N., Manukyan A.S., Rybkin V.V.** Precipitation of nickel containing particles from nickel nitrate solutions under the action of a direct current glow discharge. *ChemChemTech [Izv. Vyssh. Uchebn. Zaved. Khim. Khim. Tekhnol.].* 2022. V. 65. N 12. P. 112-118 (in Russian). DOI: 10.6060/ivkkt.20226512.6743.
19. **Смирнова К.В., Шутов Д.А., Иванов А.Н., Манукян А.С., Рыбкин В.В.** Плазменно-растворный синтез оксида цинка, допированного кадмием. *Изв. вузов. Химия и хим. технология*. 2022. Т. 65. Вып. 7. С. 28-34. **Smirnova K.V., Shutov D.A., Ivanov A.N., Manukyan A.S., Rybkin V.V.** Plasma-solution synthesis of zinc oxide doped with cadmium. *ChemChemTech [Izv. Vyssh. Uchebn. Zaved. Khim. Khim. Tekhnol.].* 2022. V. 65. N 7. P. 28-34. DOI: 10.6060/ivkkt.20226507.6629.
20. **Wang Y., Wang S., Li X., Bai P., Yan W., Yu J.** Layered inorganic cationic frameworks beyond layered double 24 hydroxides (LDHs): structures and applications. *Eur. J. Inorg. Chem.* 2020. V. 43. P. 4055–4063. DOI: 10.1002/ejic.202000710.
21. **Oliver S.R.J.** Cationic inorganic materials for anionic pollutant trapping and 26 catalysis. *Chem. Soc. Rev.* 2009. V. 38. N 7. P. 1868-1981. DOI: 10.1039/b710339p.
22. **Geng F., Y. Matsushita Y., Ma R., Xin H., Tanaka M., Izumi F., Iyi N., Sasaki T.** General Synthesis and Structural Evolution of a Layered Family of $Ln_8(OH)_{20}Cl_4{\cdot}nH_2O$ (Ln = = Nd, Sm, Eu, Gd, Tb, Dy, Ho, Er, Tm, and Y). *J. Am. Chem. Soc.* 2008. V. 130. N 48. P. 16344–16350. DOI: 10.1021/ja807050e.
23. **Liang J., Ma R., Geng F., Ebina Y., Sasaki T.** $Ln_2(OH)_4SO_4{\cdot}nH_2O$ (Ln = Pr to Tb; n ~ 2): A New Family of Layered Rare-Earth Hydroxides Rigidly Pillared by Sulfate Ions. *Chem. Mater.* 2010. V. 22. N 21. P. 6001–6007. DOI: 10.1021/cm102236n.

Поступила в редакцию 26.03.2026
Принята к опубликованию 01.04.2026

Received 26.03.2026
Accepted 01.04.2026